

Style Content Decomposition-based Data Augmentation for Domain Generalizable Medical Image Segmentation

Zhiqiang Shen^{1,2}, Peng Cao^{1,2*}, Jinzhu Yang^{1,2}, Osmar R. Zaiane³, and Zhaolin Chen^{4,5}

- ¹ School of Computer Science and Engineering, Northeastern University, Shenyang, China
- ² Key Laboratory of Intelligent Computing in Medical Image, Ministry of Education, Shenyang, China
xxszqyy@gmail.com
- ³ Alberta Machine Intelligence Institute, University of Alberta, Edmonton, Alberta, Canada
- ⁴ Monash Biomedical Imaging, Monash University, Australia
- ⁵ Department of Data Science and AI, Monash University, Australia

Abstract. Due to the domain shifts between training and testing medical images, learned segmentation models often experience significant performance degradation during deployment. In this paper, we first decompose an image into its style code and content map and reveal that domain shifts in medical images involve: **style shifts** (*i.e.*, differences in image appearance) and **content shifts** (*i.e.*, variations in anatomical structures), the latter of which has been largely overlooked. To this end, we propose **StyCona**, a **style content** decomposition-based data augmentation method that innovatively augments both image style and content within the rank-one space, for domain generalizable medical image segmentation. StyCona is a simple yet effective plug-and-play module that substantially improves model generalization without requiring additional training parameters or modifications to the segmentation model architecture. Experiments on cross-sequence, cross-center, and cross-modality medical image segmentation settings with increasingly severe domain shifts, demonstrate the effectiveness of StyCona and its superiority over state-of-the-arts. The code is available at <https://github.com/Senyh/StyCona>.

Keywords: Domain generalization · Medical image segmentation · Style code · Content map.

1 Introduction

Medical image segmentation is an essential task for computer-aided diagnosis systems. Driven by large and diverse annotated datasets, deep learning-based

* Corresponding author

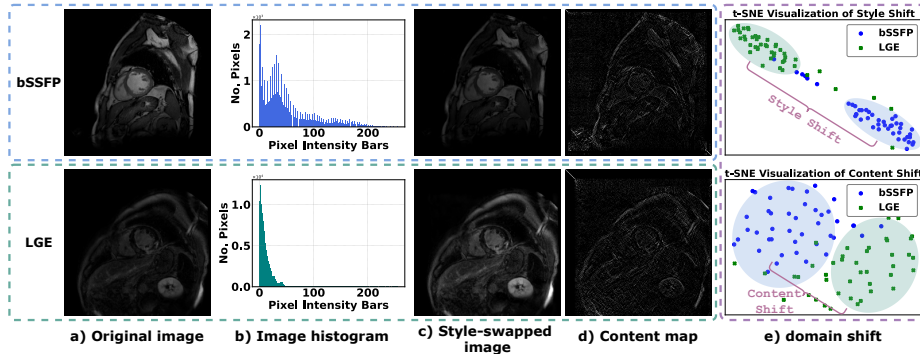


Fig. 1. Illustration of style codes and content maps for bSSFP and LGE MRI sequences: a) original images showing disparities in both style (image appearance) and content (anatomical structures), b) image histograms reflecting domain shifts in terms of pixel intensities, c) style-swapped images generated by swapping the two original images’ style codes (top: bSSFP image with LGE style; bottom: LGE image with bSSFP style), d) content maps derived from the sum of an image’s rank-one components, and e) t-SNE [10] visualization of domain shifts (top: style shift; bottom: content shift).

segmentation models have achieved remarkable progress [15,11]. However, data distribution mismatches (*a.k.a.*, domain shifts), caused by diverse imaging protocols, equipment vendors, or patient populations, *etc.*, between training and testing datasets hinder the generalizability of trained models for clinical deployment [3,19,5]. As a consensus [14,4,12], domain shifts often manifest as differences in pixel intensity [Fig. 1(b)]. To alleviate the shifts, numerous data augmentation-based domain generalization (DG) methods have been proposed to expand training data distributions and encourage segmentation models to learn domain-invariant representations across domains. Concretely, they perform style augmentation in the frequency space [18,16,9], feature space [20,4], or image space [17,12] to generate augmented data by transforming image appearance. Although such style augmentation techniques effectively expose the model to diverse style-augmented data, they fail to handle the more complex nature of domain shifts, *e.g.*, object shape variations arising from population- or pathology-related changes and the tissue-reconstruction differences caused by various imaging modalities. These shifts reflect anatomical structure discrepancies rather than naive image appearance disparities.

Understanding the underlying nature of domain shifts is crucial for designing more effective augmentation methods. Inspired by the fact that an image’s rank-one matrices correspond to its principle components, which are capable of modeling high-level statistics [2,6], we decompose an image into its style codes and content maps in the rank-one space and reveal that 1) the style codes captures the image’s appearance within an anatomical structure and 2) the content maps describe the image’s anatomical structure. To provide a clearer intuition, we visualize style-swapped images (by exchanging two images’ style codes) and

content maps in Fig. 1(c-d); it can be observed that the content maps accurately delineate the anatomical structures within the original bSSFP and LGE images, and the style-swapped images transfer appearance between each other while preserving the original anatomical structures. Based on the decomposition, we categorize domain shifts into two components [Fig. 1(e)]: 1) **style shift** (image appearance variations) indicated by the deviations between the style codes, and 2) **content shift** (anatomical structure discrepancies) reflected in the differences between the content maps. However, explicitly measuring the two types of shifts is infeasible due to unknown target domains during training. In light of the above, we identify the key issue as follows: *When only a single domain (e.g., bSSFP) is available in training data, how can we sufficiently exploit the source domain to ensure that the trained model effectively alleviate both style and content shifts for improving the segmentation performance on unseen domains (e.g., LGE)?*

Considering the limitations of previous studies, we hypothesize that *style shifts and content shifts can be mitigated through data augmentation from the aspects of style and content within the rank-one space*. Building upon this assumption, we propose a **style content** decomposition-based data **augmentation** method, termed **StyCona**, to advance domain generalizable medical image segmentation. The main idea behind StyCona is that style and content augmentation can be achieved through perturbations within the rank-one space, where 1) blending style codes enables image style augmentation, and 2) mixing content maps facilitates image content augmentation. We evaluate StyCona on three cross-domain settings with increasingly severe domain shifts: cross-sequence, cross-center, and cross-modality. Experimental results demonstrate that our StyCona is a promising solution for domain generalizable medical image segmentation and achieves state-of-the-art performance. Our contributions are as follows:

- To the best of our knowledge, this is the first work that decomposes domain shifts into style shifts and content shifts.
- We propose StyCona, a novel data augmentation paradigm within the rank-one space for domain-generalizable medical image segmentation. Our method can be easily integrated into off-the-shelf medical image segmentation backbones and effectively mitigates the two types of domain shifts.
- StyCona leads to state-of-the-art performance across a wide range of tasks and provides a compelling alternative to Fourier transformation-based, style transfer-based, and random convolution-based data augmentation methods.

2 Methodology

Through dividing domain shifts into style and content shifts, we devise the **style content** decomposition-based data **augmentation** method (**StyCona**) for domain-generalizable medical image segmentation. The main assumption behind StyCona is that the two types of shifts can be mitigated through style and content augmentations within the rank-one space. Building upon this assumption, StyCona augments image style and content by perturbing style codes and

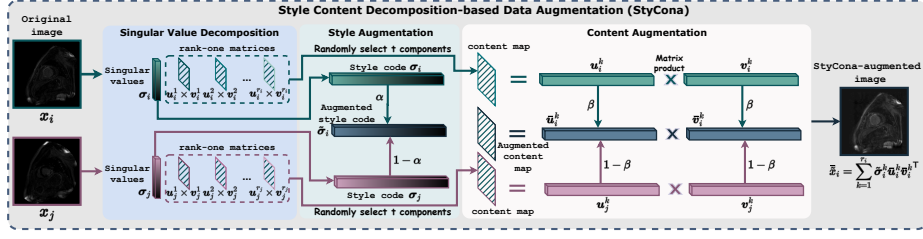


Fig. 2. The schematic diagram of the proposed **style content** decomposition-based data augmentation method (**StyCona**). StyCona includes three steps: 1) singular value decomposition, 2) style augmentation, and 3) content augmentation. x_i and x_j represent original images, and \tilde{x} denotes a StyCona-augmented sample.

content maps, respectively. This idea is realized using singular value decomposition (SVD) [8] to decompose an image into its singular values (style codes) and rank-one matrices (content maps)⁶ and then conducts 1) style augmentation by perturbing the singular values, and 2) content augmentation by perturbing the rank-one matrices [Fig. 2]. As mentioned in Section 1, style codes control the image appearance within an anatomical structure, and content maps describe the anatomical structures. From a frequency perspective, these properties align with the characteristics of frequency spectra, where amplitude spectrum controls an image’s low-level statistics (style), while phase spectrum corresponds to high-level semantics (content) [18,16]. Specifically, the StyCona algorithm comprises three components: 1) singular value decomposition, 2) style augmentation, and 3) content augmentation, which are detailed as follows.

Singular Value Decomposition. For an image x , its SVD is formulated as:

$$x = \sum_{k=1}^r \underbrace{\sigma^k}_{\text{singular value}} \underbrace{\mathbf{u}^k \mathbf{v}^{k\top}}_{\text{rank-one matrix}} \quad (1)$$

where each singular value σ^k acts as a style code and the rank-one matrix $\mathbf{u}^k \mathbf{v}^{k\top}$ serves as a content map for the subsequent style and content augmentation.

Style Augmentation. Based on our assumption, image style augmentation can alleviate style shifts (variations in image appearance). As illustrated in Fig. 2, we perform style augmentation on an image x_i by blending its **style codes** (*i.e.*, **singular values**) with those of another image x_j in an element-wise manner:

$$\tilde{\sigma}_i^k = \alpha \times \sigma_i^k + (1 - \alpha) \times \sigma_j^k \quad (2)$$

⁶ Unless otherwise specified and without causing ambiguity, we will refer to a rank-one matrix (rather than their sum) as a content map, although in our findings, the content map of an image is constituted by the sum of its rank-one matrices.

where the weight $\alpha \sim U(0, 1)$ controls the mixing strength, σ_i^k represents the k_{th} singular value of image x_i , i/j indicates the sample index and $i \neq j$. After that, a style-augmented image \tilde{x}_i can be generated using the perturbed singular values and the original singular vectors by Eq. (1).

Content Augmentation. We devise image content augmentation to mitigate content shifts (disparities in anatomical structure). This is achieved by mixing a set of t randomly selected **content maps (i.e., rank-one matrices)** from an image x_i with another set of t randomly selected content maps from a different image x_j [Fig. 2]. The perturbation to each content map is formulated as:

$$\bar{\mathbf{u}}_i^k = \beta \times \mathbf{u}_i^k + (1 - \beta) \times \mathbf{u}_j^k \quad \text{or} \quad \bar{\mathbf{v}}_i^k = \beta \times \mathbf{v}_i^k + (1 - \beta) \times \mathbf{v}_j^k \quad (3)$$

where the weight $\beta \sim U(0, 1)$ and $\mathbf{u}_{i/j}^k/\mathbf{v}_{i/j}^k$ represents the left/right singular vector of image $x_{i/j}$. Using the perturbed content maps and the original style codes, we can obtain a content-augmented image \bar{x}_i via Eq. (1).

In a nutshell, by leveraging Eq. (1)(2)(3), StyCona conducts style and content augmentation and produces an augmented image $\tilde{x}_i = \sum_{k=1}^{r_i} \tilde{\sigma}_i^k \bar{\mathbf{u}}_i^k \bar{\mathbf{v}}_i^{k\top}$.

3 Experiments and Results

We evaluate our method on three domain generalizable medical image segmentation settings with increasingly severe domain shifts: **Cross-Sequence** between the LGE and bSSFP MRI sequences on the MS-CMR dataset [21]. The segmentation labels include three structures: the right ventricle (RV), left ventricle (LV), and myocardium (MYO). **Cross-Center** between the ACDC [1] and MS-CMR [21] datasets. This setting also involves the above-mentioned three foreground classes. **Cross-Modality** between the MR and CT modalities on the MMWHS dataset [22]. This 3D segmentation task includes five foreground labels: RV, LV, MYO, left atrium (LA), and right atrium (RA). Among these settings, **one sequence/center/modality is split into the training and validation sets at a ratio of 8 : 2 (source domain), and the other serves as the test set (target domain)**. Dice similarity coefficient (DSC) and average surface distance (ASD) are utilized to evaluate segmentation performance.

Implementation Details. We conduct the experiments using PyTorch [13] on an NVIDIA A40 GPU with 48G GPU memory. All compared methods are optimized using an AdamW optimizer [7] with a fixed learning rate of $1e - 4$ during the 100/1000 training epochs for 2D/3D image segmentation tasks. U-Net [15] and V-Net [11] are employed as the baseline segmentation models for 2D and 3D image segmentation experiments, respectively. We set the number of perturbed content maps $t = 16$ (please refer to Section 3.2 for further analysis).

3.1 Comparison with State of the Arts

We extensively compared our StyCona with state-of-the-art DG methods: Fourier transformation-based approaches (amplitude swap (AS) [18], amplitude mixup

(AM) [16], and FMAug [9]), style transfer-based approaches (MixStyle [20] and TriD [4]), and random convolution-based approaches (RandConv [17] and CIDA [12])), on cross-sequence, cross-center, and cross-modality domain generalizable medical image segmentation settings. We re-implemented all the compared methods in a unified experimental setup for fair comparison. All the methods are built upon the same baseline segmentation model (U-Net for 2D and V-Net for 3D scenarios, respectively). In general, StyCona sets the state-of-the-art in all three settings both quantitatively [Table 1] and qualitatively [Fig. 3], showcasing its superiority in domain generalizable medical image segmentation.

Quantitative results. As indicated in Table 1, StyCona achieves consistent performance improvements over the compared methods among the three settings. In general, almost all the compared methods surpass the baseline model in the three settings, implying their effectiveness in overcoming style shifts. However, it is worth noting that some augmentation methods, *e.g.*, AM and TriD, yield segmentation results inferior to those of the baseline model in the bSSFP \rightarrow LGE scenario. This is because the blended high-frequency amplitude in AM and the over-mixed statistics in TriD generate augmented samples that deviate significantly from the target domain images, causing the models to be overwhelmed by spurious correlations between the augmented samples and the segmentation outcomes. For scenarios with relatively mild domain shifts and sufficient source domain data, such as the ACDC \rightarrow MS-CMR scenario, all the methods obtain comparable performance. The reasons behind this phenomenon are: 1) In such scenarios, style augmentation on source domain training data can generate augmented images that largely cover unseen target domains, and 2) the training set includes samples from diverse patients, ensuring that the segmentation models are exposed to a wide range of anatomical structures during training. In contrast, for scenarios with severe domain shifts and a limited number of training samples *e.g.*, the cross-modality setting involving both variations in image appearance and disparities in anatomical structures (arising from inherent reconstruction differences between MRI and CT, as well as population-related anatomical variations), our StyCona demonstrates its advantage in handling style and content shifts by augmenting both the style and content components of images. As shown in Table 1, due to this advantage, StyCona outperforms the second-best results by 6.68% and 17.27% in terms of DSC on the cross-modality setting. The quantitative results validate our assumption and highlight the superiority of StyCona for domain-generalizable medical image segmentation.

Qualitative results. As shown in Fig. 3, StyCona produces segmentation results with more precise object delineation. The improvement can be attributed to StyCona’s style and content augmentations, which enable the augmented samples to cover a wide range of unseen domains, thereby allowing the trained model to generate accurate segmentation maps for unseen data. In comparison, methods such as AM [16], MixStyle [20], and CIDA [12] yield relatively unsatisfactory results. AM and MixStyle rely solely on style augmentation by blending amplitude spectra and adjusting the mean and standard deviation of samples,

Table 1. Comparison with state-of-the-art methods on the cross-sequence, cross-center, and cross-modality settings. The best and second-best results are highlighted in **red** and **blue**, respectively.

Method	Cross-Sequence				Cross-Center				Cross-Modality			
	bSSFP → LGE		LGE → bSSFP		ACDC → MS-CMR		MS-CMR → ACDC		MR → CT		CT → MR	
	DSC ↑	ASD ↓	DSC ↑	ASD ↓	DSC ↑	ASD ↓	DSC ↑	ASD ↓	DSC ↑	ASD ↓	DSC ↑	ASD ↓
Baseline	65.97	6.55	76.91	3.41	75.05	8.04	66.69	8.56	13.44	43.18	14.99	27.32
AS	70.93	6.48	78.74	3.26	80.55	2.50	69.46	7.57	60.42	14.66	32.09	17.48
AM	63.89	6.44	80.07	2.46	80.86	3.02	70.08	7.86	47.01	18.99	22.51	13.83
FMAug	72.46	13.67	80.54	2.57	79.39	2.53	68.27	6.44	45.99	23.37	33.52	14.85
MixStyle	69.26	10.91	80.81	2.69	79.21	2.72	68.11	7.49	48.99	16.74	25.06	22.93
TriD	65.12	10.25	79.14	4.60	79.60	3.29	64.96	10.49	39.41	20.43	24.23	9.45
RandConv	71.90	5.65	75.17	4.27	80.43	2.65	65.50	8.33	42.24	16.30	30.89	9.25
CIDA	69.72	8.63	72.85	4.61	80.72	2.31	68.54	14.43	69.18	5.97	50.94	8.05
StyCona (ours)	73.39	4.33	81.59	2.24	80.54	2.01	71.04	5.54	75.86	4.62	68.21	6.39

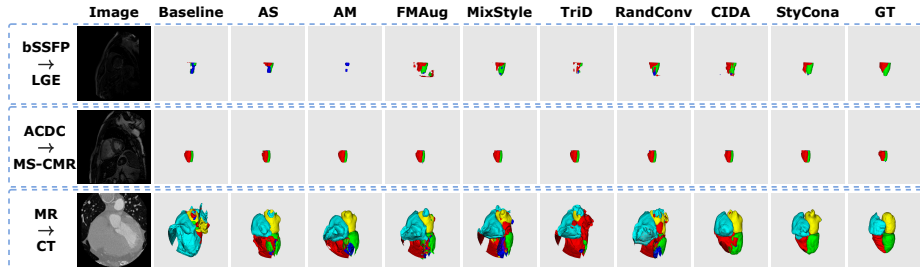


Fig. 3. Qualitative results on the bSSFP → LGE, ACDC → MS-CMR, and MR → CT scenarios. GT: ground truth.

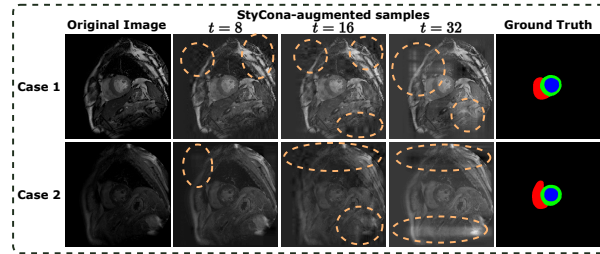
respectively. Meanwhile, the effectiveness of CIDA is limited by its simple combination of style-perturbed samples using randomly generated correlation maps, which inadequately address variations in anatomical structures. These qualitative results, consistent with the quantitative performance, further demonstrate the effectiveness of our approach.

3.2 Ablation Study

Effectiveness of each component. In Table 2, we present ablation experiments to analyze the contributions of each component of StyCona. These experiments were conducted under the cross-sequence setting. The results reveal a consistent trend: segmentation performance improves as the proposed style and content augmentation components are progressively integrated into our method. Specifically, the baseline model (*i.e.*, U-Net) performs relatively unsatisfactorily on the target domain, as it tends to learn domain-specific decision rules based on source domain data. Then, the segmentation performance increases by a large gap when the style augmentation operation is introduced, effectively mitigating style shifts, which are an essential part of domain shifts in these scenarios. In

Table 2. Ablation study of the proposed method on the cross-sequence setting. The best results are highlighted in **bold**.

Method	StyCona		bSSFP \rightarrow LGE		LGE \rightarrow bSSFP	
	Style augmentation	Content augmentation	DSC \uparrow	ASD \downarrow	DSC \uparrow	ASD \downarrow
Baseline			65.97	6.55	76.91	3.41
Baseline + Style	\checkmark		68.98	3.20	80.45	2.40
Baseline + Content		\checkmark	72.31	5.16	81.17	2.43
Baseline + Style + Content	\checkmark	\checkmark	73.39	4.33	81.59	2.24

**Fig. 4.** StyCona-augmented samples with different numbers of perturbed content maps ($t = 8$, $t = 16$, and $t = 32$) for two randomly selected original images. The orange dashed circles highlight some content-perturbed regions.

contrast, the improvement is more significant, with an increase of over 7% in DSC, when only the content augmentation component is introduced to address the content shifts, another key aspect of domain shifts. Finally, by incorporating both the style and content augmentation modules to address variations in image appearance and differences in anatomical structures, our final method achieves the best performance with DSC of 73.39% and 81.59% on the bSSFP \rightarrow LGE and LGE \rightarrow bSSFP scenarios, respectively. This result demonstrates the effectiveness of each component and validates our assumption that style and content augmentations can alleviate the two types of domain shifts.

Label Invariance. According to Eq. (1)(2)(3), perturbing the singular values alters only an image’s style without affecting its target shape corresponding to segmentation labels. On the other hand, perturbing t randomly selected rank-one matrices causes changes in image content (*e.g.*, background tissues or target object-related boundaries), which is the goal of our method to enhance the robustness of segmentation models to anatomical structure variations. Fig. 4 shows the StyCona-augmented samples with varying numbers of perturbed content maps ($t = 8, 16, 32$). Compared with the original images, the augmented images with $t = 8, 16$ exhibit variations in overall image appearance and regional anatomical structures while remaining consistent with the ground truth segmentation labels. In contrast, at $t = 32$, excessive noise is introduced into certain target boundaries, which may alter the ground truth. In light of this, we set $t = 16$ in StyCona to balance the perturbation strength with the invariance of segmentation labels and ensure label consistency after augmentation.

4 Conclusion

We propose StyCona, a novel data augmentation method for domain generalizable medical image segmentation. Our findings reveal that an image’s singular values function as style codes, governing its appearance, while its rank-one matrices serve as content maps, determining its anatomical structure. Domain shifts are then categorized into style and content shifts *w.r.t.* deviations in style codes and content maps, respectively. StyCona perturbs style codes for style augmentation and blends content maps for content augmentation. Extensive experiments on three cross-domain settings demonstrate that StyCona is a promising data augmentation technique for domain-generalizable medical image segmentation.

Acknowledgments. This work was supported by the National Natural Science Foundation of China (No.62076059, No.U22A2022), the Science and Technology Joint Project of Liaoning Province (2023JH2/101700367), the Fundamental Research Funds for the Central Universities (N2424010-7), and the China Scholarship Council (202406080040).

References

1. Bernard, O., Lalande, A., Zotti, C., Cervenansky, F., Yang, X., Heng, P.A., Cetin, I., Lekadir, K., Camara, O., Ballester, M.A.G., et al.: Deep learning techniques for automatic mri cardiac multi-structures segmentation and diagnosis: is the problem solved? *IEEE transactions on medical imaging* **37**(11), 2514–2525 (2018)
2. Candès, E.J., Li, X., Ma, Y., Wright, J.: Robust principal component analysis? *Journal of the ACM (JACM)* **58**(3), 1–37 (2011)
3. Castro, D.C., Walker, I., Glocker, B.: Causality matters in medical imaging. *Nature Communications* **11**(1), 3673 (2020)
4. Chen, Z., Pan, Y., Ye, Y., Cui, H., Xia, Y.: Treasure in distribution: a domain randomization based multi-source domain generalization for 2d medical image segmentation. In: *International Conference on Medical Image Computing and Computer-Assisted Intervention*. pp. 89–99. Springer (2023)
5. Guan, H., Liu, M.: Domain adaptation for medical image analysis: a survey. *IEEE Transactions on Biomedical Engineering* **69**(3), 1173–1185 (2021)
6. Kim, K.I., Franz, M.O., Scholkopf, B.: Iterative kernel principal component analysis for image modeling. *IEEE transactions on pattern analysis and machine intelligence* **27**(9), 1351–1366 (2005)
7. Kingma, D.P., Ba, J.: Adam: A method for stochastic optimization. In: *International Conference on Learning Representations* (2015)
8. Klema, V., Laub, A.: The singular value decomposition: Its computation and some applications. *IEEE Transactions on automatic control* **25**(2), 164–176 (1980)
9. Li, H., Li, H., Zhao, W., Fu, H., Su, X., Hu, Y., Liu, J.: Frequency-mixed single-source domain generalization for medical image segmentation. In: *International Conference on Medical Image Computing and Computer-Assisted Intervention*. pp. 127–136. Springer (2023)
10. Van der Maaten, L., Hinton, G.: Visualizing data using t-sne. *Journal of machine learning research* **9**(11) (2008)
11. Milletari, F., Navab, N., Ahmadi, S.A.: V-net: Fully convolutional neural networks for volumetric medical image segmentation. In: *2016 fourth international conference on 3D vision (3DV)*. pp. 565–571. Ieee (2016)

12. Ouyang, C., Chen, C., Li, S., Li, Z., Qin, C., Bai, W., Rueckert, D.: Causality-inspired single-source domain generalization for medical image segmentation. *IEEE Transactions on Medical Imaging* **42**(4), 1095–1106 (2022)
13. Paszke, A., Gross, S., Massa, F., Lerer, A., Bradbury, J., Chanan, G., Killeen, T., Lin, Z., Gimelshein, N., Antiga, L., et al.: Pytorch: An imperative style, high-performance deep learning library. *Advances in neural information processing systems* **32** (2019)
14. Pei, C., Wu, F., Huang, L., Zhuang, X.: Disentangle domain features for cross-modality cardiac image segmentation. *Medical Image Analysis* **71**, 102078 (2021)
15. Ronneberger, O., Fischer, P., Brox, T.: U-net: Convolutional networks for biomedical image segmentation. In: *Medical image computing and computer-assisted intervention—MICCAI 2015: 18th international conference, Munich, Germany, October 5–9, 2015, proceedings, part III* 18. pp. 234–241. Springer (2015)
16. Xu, Q., Zhang, R., Zhang, Y., Wang, Y., Tian, Q.: A fourier-based framework for domain generalization. In: *Proceedings of the IEEE/CVF Conference on Computer Vision and Pattern Recognition*. pp. 14383–14392 (2021)
17. Xu, Z., Liu, D., Yang, J., Raffel, C., Niethammer, M.: Robust and generalizable visual representation learning via random convolutions. In: *International Conference on Learning Representations* (2021)
18. Yang, Y., Soatto, S.: Fda: Fourier domain adaptation for semantic segmentation. In: *Proceedings of the IEEE/CVF conference on computer vision and pattern recognition*. pp. 4085–4095 (2020)
19. Zhou, K., Liu, Z., Qiao, Y., Xiang, T., Loy, C.C.: Domain generalization: A survey. *IEEE Transactions on Pattern Analysis and Machine Intelligence* **45**(4), 4396–4415 (2022)
20. Zhou, K., Yang, Y., Qiao, Y., Xiang, T.: Domain generalization with mixstyle. In: *International Conference on Learning Representations* (2021)
21. Zhuang, X.: Multivariate mixture model for myocardial segmentation combining multi-source images. *IEEE transactions on pattern analysis and machine intelligence* **41**(12), 2933–2946 (2018)
22. Zhuang, X., Li, L., Payer, C., Štern, D., Urschler, M., Heinrich, M.P., Oster, J., Wang, C., Smedby, Ö., Bian, C., et al.: Evaluation of algorithms for multi-modality whole heart segmentation: an open-access grand challenge. *Medical image analysis* **58**, 101537 (2019)